THE IMAGINARY PART OF THE NUCLEON SELF-ENERGY IN HOT NUCLEAR MATTER

L. Alvarez-Ruso[a], P. Fernández de Córdoba[b] and E. Oset[a]

[a] *Departamento de Física Teórica and IFIC*
Centro Mixto Universidad de Valencia-CSIC
Valencia, Spain

[b] *Departamento de Matemática Aplicada*
Universidad Politécnica de Valencia
Valencia, Spain

Abstract

A semiphenomenological approach to the nucleon self-energy in nuclear matter at finite temperatures is followed. It combines elements of Thermo Field Dynamics for the treatment of finite temperature with a model for the self-energy, which evaluates the second order diagrams taking the needed dynamics of the NN interaction from experiment. The approach proved to be accurate at zero temperature to reproduce $Im\Sigma$ and other properties of nucleons in matter. In the present case we apply it to determine $Im\Sigma$ at finite temperatures. An effective NN cross section is deduced which can be easily used in analyses of heavy ion reactions.

1 Introduction

The imaginary part of the nucleon self-energy Σ has been the subject of intense research in the past [1]. However, these studies have been done at zero temperature, of relevance for physical processes involving nucleon-nucleus scattering. On the other hand, in heavy ion collisions, through multiple collisions of the nucleons, one reaches conditions roughly similar to those of a thermal bath at finite temperature [2]. The imaginary part of the nucleon self-energy in such a bath is an important magnitude which governs processes of nucleon emission, particle production and, in principle, most of the nuclear processes occurring during heavy ion collisions, including the rate of thermalization.

The many body field theoretical treatment at finite temperature becomes, however, technically more involved than at $T = 0$. At the root of it lies the fact that particle annihilation operators do not give a vanishing result when applied to the ground state of the system, which is now a thermal distribution. This does not allow one to use the Wick theorem to generate the Feynman diagrammatic perturbation expansion, as we know for many body systems at $T = 0$, or in ordinary Quantum Field Theory in the absence of a medium. Yet, even if more complicated, the methods to deal with it are available. The traditional approach has been the one of the imaginary time formalism [3, 4], although lately the new method in real time formalism known as Thermo Field Dynamics [5, 6] is proving quite efficient and becomes more and more widely used. A recent review on Thermo Field Dynamics with some applications to nuclear matter looking at collective modes and delta propagation in matter is presented in ref. [7]. A covariant formalism at finite temperature unifying the good features of the two formalisms is presented in ref. [8], with some application to nuclear matter within the relativistic Walecka model [9].

Detailed analyses of nucleon properties along the lines of ref. [1] are available at finite, but small temperatures $T \leq 10\, MeV$ [10, 11]. Neither of the two approaches mentioned above is followed, but instead the smallness of the temperature justifies some approximations by means of which one finally follows the steps at $T = 0$ substituting the Pauli distribution $n(\vec{k})$ (1 for $|\vec{k}| < k_F$, 0 for $|\vec{k}| > k_F$) by the thermal distribution

$$n(k^0) = [1 + exp(\frac{k^0 - \mu}{k_B T})]^{-1} \tag{1}$$

with k_B the Boltzmann constant, $k^0 = \varepsilon(\vec{k})$ the nucleon energy and μ the chemical potential. The results of [10] are improved in [11] by considering the correlation diagrams which lead to a large contribution to $Im\Sigma$ at momenta below the Fermi momentum. Similar steps are followed in ref. [12] to deal with the propagation of the Δ at finite temperatures.

The appeal of Thermo Field Dynamics is that one can continue to use Wick's theorem and the Feynman diagrammatic approach as at $T = 0$. The price is the introduction of an auxiliary field by means of which one constructs

a field doublet; the propagators become 2×2 matrices and the Feynman rules are now algebraic operational rules in the space of 2×2 matrices.

In the present work we shall evaluate the imaginary part of the nucleon self-energy at finite temperature. In doing so we shall be following closely the steps of ref. [13], where $Im\Sigma$ was evaluated for nuclear matter at $T = 0$. The approach used in [13] was semiphenomenological, much in line with usual approximations done in the treatment of heavy ion collisions where the results obtained here are bound to be of relevance. The approach of [13] evaluated correctly the second order nucleon self-energy diagrams but bypassed the use of an explicit NN potential. Instead, it used the fact that the sum of ladder diagrams in the low density limit provides the NN scattering t matrix, and its modulus squared, which appears in the evaluation of $Im\Sigma$, is related to the NN cross section. Hence the experimental cross section was used as input and the low density theorem [14, 15] was automatically fulfilled. This theorem states that, as the nuclear density goes to zero, one has

$$Im\Sigma_{\rho\to 0} = -\frac{1}{2}\ \sigma_{tot}\ v\ \rho \tag{2}$$

where v is the velocity of the nucleon in the rest frame of the Fermi sea and σ_{tot} the total NN cross section. Long range correlations were also considered by means of an RPA sum with a phenomenological particle-hole interaction acting in the spin-isospin transverse channel. The approach proved to be numerically quite successful by comparing the results with those of elaborate and time consuming many body approaches like those of refs. [16, 17]. Spectral functions and occupation numbers were also evaluated in [13] and were very similar to those obtained in other successful many body approaches with special emphasis in selfconsistency [18].

As with respect to the finite temperature treatment, we use the Thermo Field Dynamics approach by following the formalism, normalization and rules of ref. [19], where a comprehensive and practical extract of this method is presented.

2 Finite temperature formalism for the nucleon self-energy

By following ref. [19] we have the thermal doublet for the nucleon field

$$\psi^{(a)}(x) \equiv \left\{ \begin{array}{c} \psi(x) \\ i\ {}^t\tilde{\psi}^\dagger \end{array} \right\} \tag{3}$$

where $\psi(x)$ is the ordinary nucleon field and $\tilde{\psi}$ a support field for the formalism (t means the transposition with respect to the spinor index and $\dagger$ stands for conjugate). The thermal propagator is now defined as

$$iG^{(a,b)}(x_1, x_2) =< 0(\beta)|T[\psi^{(a)}(x_1)\bar{\psi}^{(b)}(x_2)]|0(\beta) > \tag{4}$$

where $|0(\beta)>$ is the state transformed from the vacuum by a Bogoliubov unitary transformation, and which has the property that the expectation value of an operator in this state is equivalent to its thermal average with the distribution of eq. (1). Hence the component of the Green's function, $G^{(11)}$, is the proper thermal average of the ordinary Green's function.

The thermal free propagator, to be used in perturbation theory in the nonrelativistic approximation which we shall follow here, is given by

$$G^{0\,(ab)}(p) = G_F^{0\,(ab)}(p) + G_D^{0\,(ab)}(p) \tag{5}$$

with

$$G_F^{0\,(ab)}(p) = \begin{pmatrix} G_F^0(p) & 0 \\ 0 & G_F^{0*}(p) \end{pmatrix} ; \, G_F^0(p) = \frac{1}{p^0 - \varepsilon(\vec{p}) + i\epsilon} \tag{6}$$

$$G_D^{0\,(ab)}(p) = 2\pi i \delta(p^0 - \varepsilon(\vec{p})) \begin{pmatrix} sin^2\theta_{p^0} & \frac{1}{2} sin 2\theta_{p^0} \\ \frac{1}{2} sin 2\theta_{p^0} & -sin^2\theta_{p^0} \end{pmatrix} \tag{7}$$

$$cos\theta_{p^0} = \frac{1}{(1+e^{-x})^{1/2}} \, ; \, sin\theta_{p^0} = \frac{e^{-x/2}}{(1+e^{-x})^{1/2}} \, ; x = \frac{p^0 - \mu}{k_B T} \tag{8}$$

$$sin^2\theta_{p^0} = \frac{1}{e^x + 1} = n(p^0) \tag{9}$$

This Green's function is in addition diagonal in spin but we omit the spin indices for simplicity.

An alternative way of writing this propagator which is also suited to write the exact propagator is

$$G^{0(ab)}(p) = \left[U_F(p^0) \begin{pmatrix} G_F^0(p) & 0 \\ 0 & G_F^{0*}(p) \end{pmatrix} U_F^{-1}(p^0) \right]^{(ab)} \tag{10}$$

with

$$U_F(p^0) = \begin{bmatrix} cos\theta_{p^0} & sin\theta_{p^0} \\ -sin\theta_{p^0} & cos\theta_{p^0} \end{bmatrix} \tag{11}$$

and the exact propagator can be cast as

$$G^{(ab)}(p) = U_F(p^0) \begin{pmatrix} [p^0 - \varepsilon(\vec{p}) - \bar{\Sigma}(p)]^{-1} & 0 \\ 0 & [p^0 - \varepsilon(\vec{p}) - \bar{\Sigma}^*(p)]^{-1} \end{pmatrix} U_F^{-1}(p^0) \tag{12}$$

with $\varepsilon(\vec{p})$ the kinetic energy of the particle and

$$\begin{aligned} Re\bar{\Sigma}(p) &= Re\Sigma^{(11)}(p) \\ Im\bar{\Sigma}(p) &= Im\Sigma^{(11)}(p)/cos2\theta_{p^0} \end{aligned} \tag{13}$$

In particular the $G^{0(11)}(p)$ component has an intuitive form given by

$$G^{0(11)}(p) = \frac{1 - sin^2\theta_{p^0}}{p^0 - \varepsilon(\vec{p}) - \bar{\Sigma}} + \frac{sin^2\theta_{p^0}}{p^0 - \varepsilon(\vec{p}) - \bar{\Sigma}^*} \tag{14}$$

which in the limit of $T = 0$ reproduces the standard form of the nucleon propagator in a Fermi sea.

Hence in order to obtain the self-energy $\bar{\Sigma}(p)$ which renormalizes the nucleon propagator, only the thermal component $\Sigma^{(11)}$ needs to be evaluated. In the next section we show the approximation scheme that we follow to evaluate this magnitude.

3 Semiphenomenological model for Σ

This section follows closely ref. [13]. The generic Feynman diagram which we evaluate is the one in fig. 1, where the nucleon propagator in each of the baryonic lines is given by eq. (5). Note that in the limit of $T = 0$, and with the conventional separation of particles and holes, the usual polarization (fig. 2a) and correlation (fig. 2b) graphs which lead to $Im\Sigma$ [11] are automatically generated (together with other two graphs with the interaction lines crossed which do not contribute to $Im\Sigma$).

In fig. 1 the indices a,b,c,d in the vertices are thermal indices. We are interested in $\Sigma^{(11)}$ and hence $a = b = 1$. Assuming for the moment the interaction lines to correspond to meson exchange, and considering also that no such mesons are present in the ground state of our many body fermionic system, the meson propagator would be diagonal in the thermal indices and hence $c = d = 1$.

We thus must evaluate the polarization function $\Pi^{(11)}(q)$

$$\Pi^{(11)}(q) = -4i \int \frac{d^4p}{(2\pi)^4} \;\; G^{0\,(11)}(p) \;\; G^{0\,(11)}(p+q) \tag{15}$$

where the factor 4 takes into account the sum over spin and isospin.

Once again in the limit of $T = 0$, this polarization would account for the two diagrams in fig. 3, which are those accounted for by means of the Lindhard function [4].

By using $G^{0\,(a,b)}$ from eqs. (6,7) the p^0 integration can be easily performed and one obtains

$$\Pi^{(11)}(q) = 4 \int \frac{d^3p}{(2\pi)^3} \left\{ \frac{sin^2\theta_{\varepsilon(\vec{p})} cos^2\theta_{\varepsilon(\vec{p}+\vec{q})}}{q^0 + \varepsilon(\vec{p}) - \varepsilon(\vec{p}+\vec{q}) + i\epsilon} + \frac{sin^2\theta_{\varepsilon(\vec{p}+\vec{q})} cos^2\theta_{\varepsilon(\vec{p})}}{-q^0 - \varepsilon(\vec{p}) + \varepsilon(\vec{p}+\vec{q}) + i\epsilon} \right\} \tag{16}$$

Next we evaluate $\Sigma^{(11)}$ corresponding to fig. 1

$$\Sigma^{(11)}(k) = i \int \frac{d^4q}{(2\pi)^4} \;\; V^2(q) \;\; \Pi^{(11)}(q) \;\; G^{0\,(11)}(k-q) \tag{17}$$

where $V(q)$ would take into account the interaction due to the hypothetical meson exchange.

Here again we follow the steps of ref. [13] and sum the ladder diagrams which would replace $V(q)$ by the scattering t matrix. (Note that medium corrections to t which would appear in the medium G-matrix are taken explicitly into account to second order with the structure of the diagram). We shall continue to use the same t matrix here. The studies of refs. [10, 11, 20] show indeed little dependence of the effective interaction on the temperature.

In order to evaluate $Im\Sigma^{11)}$ from eq. (17) a Wick rotation was made in ref. [13] which allows one to express $Im\Sigma^{(11)}$ in terms of $Im\Pi^{(11)}$. This is however not possible here because $\Pi^{(11)}$ from eq. (16) has overlapping cuts in the upper and lower half planes of the complex plane (unlike at $T = 0$ where the cuts are confined to the second and fourth quadrant). However, an explicit evaluation of $Im\Sigma^{(11)}$ is possible by first performing the q^0 integral in eq. (17) and then evaluating the imaginary part, with the result

$$\begin{aligned} Im\Sigma^{(11)}(k) = -4\pi \int \tfrac{d^3q}{(2\pi)^3} \int \tfrac{d^3p}{(2\pi)^3} |t|^2 \delta(k^0 + \varepsilon(\vec{p}) - \varepsilon(\vec{k} - \vec{q}) - \varepsilon(\vec{p} + \vec{q})) \\ \cdot \left\{ cos^2\theta_{\varepsilon(\vec{k}-\vec{q})} cos^2\theta_{\varepsilon(\vec{p}+\vec{q})} sin^2\theta_{\varepsilon(\vec{p})} - sin^2\theta_{\varepsilon(\vec{k}-\vec{q})} sin^2\theta_{\varepsilon(\vec{p}+\vec{q})} cos^2\theta_{\varepsilon(\vec{p})} \right\} \end{aligned} \tag{18}$$

The spin-isospin averaged value of $|t|^2$ assumed in eq. (18) is then replaced by $4\pi\sigma_{NN}/M^2$, where M is the nucleon mass and σ_{NN} the spin-isospin averaged NN elastic cross section. Since pion production is not explicitly taken into account, this restricts us below the pion production threshold. The final step in ref. [13] is to consider the polarization or RPA corrections to the interaction.

The consideration of the polarization was an important ingredient in ref. [13], which reduced $Im\Sigma$ particularly at small energies, and provided results similar to those found in refs. [16, 17]. We implement it here too. For this purpose we need to evaluate $\Pi^{(11)}(q)$, both the real and imaginary part, which cares about ph excitation, and $\Pi^{(11)}_\Delta(q)$, the equivalent term accounting for Δh excitation. At $T = 0$ these quantities are the familiar Lindhard functions $U_N(q), U_\Delta(q)$, respectively, used in ref. [13].

The real part of $U_N(q)$, unlike $ImU_N(q)$, is not affected by Pauli blocking [4], hence finite temperature, which modifies occupation numbers, has not much of a consequence in the change of $ReU_N(q)$. On the other hand there is no Pauli blocking in the Δh excitation since we do not have a Fermi sea of Δ's. For these reasons we keep $Re\Pi^{(11)}$ and $\Pi^{(11)}_\Delta$ at finite temperatures equal to $ReU_N(q), U_\Delta(q)$ at zero temperature. However, we evaluate $Im\Pi^{(11)}(q)$ from eq. (16) at finite temperature. The reason is that keeping $Im\Pi^{(11)} \neq 0$ is important in order to avoid singularities coming from poles of zero sound (q^0 proportional to $|\vec{q}|$ at small energies) which are strongly dumped at finite T.

The expression for $Im\Pi^{(11)}$ obtained from eq. (16) is given by

$$\begin{aligned} Im\Pi^{(11)}(q^0, q) = -\tfrac{1}{\pi} \quad \int_{p_{min}}^{\infty} dp \tfrac{mp}{q} \{ sin^2\theta_{\varepsilon(\vec{p})} + sin^2\theta_{\varepsilon(\vec{p})+q^0} \\ -2 sin^2\theta_{\varepsilon(\vec{p})} sin^2\theta_{\varepsilon(\vec{p})+q^0} \} \end{aligned} \tag{19}$$

where

$$p_{min} = \frac{m}{p}\,|q^0 - \frac{\vec{q}^{\,2}}{2m}| \tag{20}$$

The polarization correction replaces the interaction by the induced interaction [21] (see eq. (15) of ref. [13]). Furthermore, we can perform some trivial integrals and eliminate the δ function with the final result

$$\begin{array}{l} Im\Sigma^{(11)}(k) = -\frac{\sigma_{NN}}{M\pi^2}\int_0^\infty qdq\int_{-1}^1 dcos\theta\int_0^\infty pdp\,\Theta(1-A^2) \\ \cdot\frac{1}{|1-V_t(q)U(q)|^2}\big|_{q^0=k^0-\varepsilon(\vec{k}-\vec{q})} \\ \cdot\left\{cos^2\theta_{\varepsilon(\vec{k}-\vec{q})}cos^2\theta_{\varepsilon(\vec{p}+\vec{q})}sin^2\theta_{\varepsilon(\vec{p})} - sin^2\theta_{\varepsilon(\vec{k}-\vec{q})}sin^2\theta_{\varepsilon(\vec{p}+\vec{q})}cos^2\theta_{\varepsilon(\vec{p})}\right\} \end{array} \tag{21}$$

where $V_t(q)$ is the transverse part of the spin-isospin interaction and $U(q) = \Pi^{(11)}(q) + \Pi^{(11)}_\Delta(q)$. The arguments leading to this modifications and expressions for $V_t(q)$ and $U_N(q)$, $U_\Delta(q)$ can be found in ref. [13] and we do not repeat them here. Furthermore the angle in the integral over $cos\theta$ in eq. (21) is the angle between $\vec{q}$ and $\vec{k}$. The magnitude A in the argument of the step function is given by

$$A = \frac{M}{pq}\left\{k^0 - \frac{k^2}{2M} - \frac{q^2}{M} + \frac{kqcos\theta}{M}\right\} \tag{22}$$

with k, q the modulus of $\vec{k}$ and $\vec{q}$ respectively.

The value of the chemical potential μ as a function of the density and T is obtained, as usually done, by the normalization condition

$$\rho = 4\int\frac{d^3k}{(2\pi)^3}\frac{1}{1+exp[(\varepsilon(k)-\mu)/k_BT]} \tag{23}$$

Eq. (21) provides $Im\Sigma^{(11)}$ as a function of $k^0, \vec{k}$. In the next section we show the results which we obtain for this quantity.

4 Results and discussion

In fig. 4 we show the results of $-Im\bar{\Sigma}$ at $T = 0$ for two densities, ρ_0 $(0.17\,fm^{-3})$ and $\rho_0/2$, obtained with the present formalism in the limit of $T = 0$. The results agree with those in ref. [13] calculated with the $T = 0$ formalism and also with those of the microscopic approach of ref. [16]. Note that since only kinetic energies are used as input to evaluate $\Sigma^{(11)}$, the value of μ is referred to an origin of energies at $|\vec{k}| = 0$. We are not interested in $Re\Sigma$ and to overcome the arbitrary origin of energies we plot the magnitudes in terms of $\omega - \mu$ ($\omega \equiv k^0$). In fig. 4, $|\vec{k}|$ is taken at the value $\sqrt{2M\omega}$. This justifies small differences with ref. [13] where the value of $|\vec{k}|$ satisfying the dispersion relation between $|\vec{k}|$ and ω was taken. In fig. 4 we observe the

typical features that $Im\bar{\Sigma}$ is proportional to $(\omega-\mu)^2$. In the calculations we find that $Im\Sigma^{(11)}$ changes sign at $\omega=\mu$, with $Im\Sigma^{(11)}<0$ for $\omega>\mu$. In this case

$$\begin{aligned} cos2\theta_{k^0} &= 1-2sin^2\theta_{k^0} \\ &= 1-2n(k^0)_{T=0} = \left\{ \begin{array}{cc} -1 & \omega<\mu \\ 1 & \omega>\mu \end{array} \right. \end{aligned} \tag{24}$$

and then

$$Im\bar{\Sigma} = \frac{Im\Sigma^{11}}{cos^2\theta_{k^0}} = -|Im\Sigma^{11}| \tag{25}$$

The Green's function $G^{(11)}$, by using eq. (12), will then be

$$\frac{\Theta(\omega-\mu)}{k^0-\varepsilon(\vec{k})-Re\Sigma^{(11)}(k)+i|Im\Sigma^{(11)}|}+\frac{\Theta(\mu-\omega)}{k^0-\varepsilon(\vec{k})-Re\Sigma^{(11)}(k)-i|Im\Sigma^{(11)}|}$$

$$\equiv \frac{1}{k^0-\varepsilon(\vec{k})-\Sigma^{(11)}} \tag{26}$$

as it should be.

In fig. 5 we plot $Im\Sigma^{(11)}$ at $\rho=\rho_0$ as a function of $\omega-\mu$, with $|\vec{k}|=\sqrt{2M\omega}$ and μ calculated from eq. (23). As can be seen in the figure, $Im\Sigma^{(11)}$ is always zero at $\omega=\mu$. However, $Im\bar{\Sigma}(\mu,k)$ is different from zero at finite temperatures, contrary to the situation at $T=0$ where it is zero. In order to envisage this we see that the evaluation of $Im\bar{\Sigma}$ from eq. (13) involves a fraction of the type 0/0 which we determine using l'Hôpital rule and find

$$Im\bar{\Sigma}(\mu,k) = \lim_{k^0\to\mu}\frac{Im\Sigma^{(11)}(k^0,k)}{1-2n(k^0)} = 2k_BT\frac{d}{dk^0}Im\Sigma^{(11)}(k^0,k)|_{k^0=\mu} \tag{27}$$

We can see that $Im\bar{\Sigma}(\mu,k)$ vanishes at $T=0$, as we already said.

In fig. 6,7,8 we show the results for $-Im\bar{\Sigma}$ as a function of $\omega-\mu$ for different temperatures, calculated for three different densities, $\rho_0/2, \rho_0$ and $2\rho_0$. We can appreciate that as T increases $-Im\bar{\Sigma}$ also increases in all the range of energies calculated there. We should note that in evaluating $Im\bar{\Sigma}$, the factor $cos2\theta_{k^0}$ appearing in the denominator of eq. (13) is very important and makes $Im\bar{\Sigma}\neq 0$ at $T\neq 0$ for all the range of energies, while $Im\Sigma^{(11)}$ passed through zero. This is a genuine temperature dependent property which would be lost if a $T=0$ formalism, changing the Fermi distribution by the thermal distribution of eq. (1), were used.

At this point it is interesting to compare our results for $Im\bar{\Sigma}$ with those which we would obtain using standard formulae of Fermi-liquid theory [22]. The formula used there in our notation for $Im\bar{\Sigma}$, removing the cut off in the integral, would be given by eq. (18) changing the minus sign in the curled

bracket (cos^2 and sin^2 terms) by a positive sign. Instead our formula for $Im\bar{\Sigma}$ uses eq. (18) with a minus sign (which provides $Im\Sigma^{(11)}$) and then we divide by $cos2\theta_{po}$ (as shown in eq. (13)) in order to obtain $Im\bar{\Sigma}$. The same prescription would be taken if one uses instead eq. (21) which incorporates the effects of polarization.

It is easy to see that at $T = 0$ both formulae are identical. Indeed for $\omega > \mu$ only the first term in the curled bracket of eq. (18) (or (21)) (the one with $cos^2cos^2sin^2$) contributes, while for $\omega < \mu$ only the second term in the bracket (the one with $sin^2sin^2cos^2$) contributes. Then when dividing $Im\Sigma^{(11)}$ by $cos2\theta_{p^0}$, given by eq. (24), we obtain a formula for $Im\bar{\Sigma}$ given by eq. (18) where the minus sign in the curled bracket is changed to a positive sign, exactly the formula used in Fermi-liquid theory [22].

The identity of the two formulae holds, however, at any temperature. This can be seen analytically using eqs. (8) for $sin\theta, cos\theta$ and x, hence

$$\begin{aligned}
& \frac{(cos^2\theta_{\varepsilon_1}cos^2\theta_{\varepsilon_2}sin^2\theta_{\varepsilon_3} - sin^2\theta_{\varepsilon_1}sin^2\theta_{\varepsilon_2}cos^2\theta_{\varepsilon_3})}{cos2\theta_{k^0}}\delta(k^0 + \varepsilon_3 - \varepsilon_1 - \varepsilon_2) \\
= & \frac{1}{k_BT}\frac{e^{x_3}[e^{(x_1+x_2-x_3)} - 1]}{(1+e^{x_1})(1+e^{x_2})(1+e^{x_3})}\frac{e^{x_{k^0}}+1}{e^{x_{k^0}}-1}\delta(x_{k^0} + x_3 - x_1 - x_2) \\
= & \frac{1}{k_BT}\frac{e^{x_1}e^{x_2} + e^{x_3}}{(1+e^{x_1})(1+e^{x_2})(1+e^{x_3})}\delta(x_{k^0} + x_3 - x_1 - x_2) \\
= & (cos^2\theta_{\varepsilon_1}cos^2\theta_{\varepsilon_2}sin^2\theta_{\varepsilon_3} + sin^2\theta_{\varepsilon_1}sin^2\theta_{\varepsilon_2}cos^2\theta_{\varepsilon_3})\delta(k^0 + \varepsilon_3 - \varepsilon_1 - \varepsilon_2)
\end{aligned} \tag{28}$$

where the constraints of the δ-function have been used in the second step. This is an interesting finding which stresses the value of the results obtained in Fermi-liquid theory based on the concept of quasiparticles, by comparison to a method in principle more microscopic, like the one used here.

Next we would like to extract a practical magnitude from these results which can be used in calculations of heavy ion collisions. Recall that in the semiclassical approach one has

$$Im\bar{\Sigma} = -\frac{1}{2}\ \sigma_{NN}\ v\ \rho \tag{29}$$

One can then define an effective NN nucleon-nucleon cross section at different T and ρ by means of

$$\sigma_{NN}^{eff} = -2\ \frac{Im\bar{\Sigma}}{v\rho} \tag{30}$$

as done in ref. [23], where $\sigma_{NN}^{eff}\ \rho$ defines a probability of collision per unit length for the nucleon. In order to facilitate the use of this magnitude we have parameterized $v\sigma_{NN}^{eff}$, with $v = |\vec{k}|/M$ for the different densities and temperatures evaluated here. We take the following functional form

$$v\sigma_{NN}^{eff} = \sum_{n=0}^{4} a_n(\rho, T)\ \omega^n \tag{31}$$

where ω is the nucleon kinetic energy, $\vec{k}^2/2M$. The fit is valid for values of $\omega > \mu$ in figures 6,7,8. The coefficients $a_n(\rho, T)$ are given in tables I,II,III. One can obtain $v\sigma_{NN}^{eff}$ for intermediate values of ρ and T interpolating between the values of $v\sigma_{NN}^{eff}$ given by eq. (29).

5 Conclusions

We have used a model to evaluate $Im\bar{\Sigma}$ for a nucleon in nuclear matter at finite temperatures, which combines the formalism of Thermo Field Dynamics with empirical magnitudes of the NN interaction. This model at $T = 0$ coincides with a semiphenomenological approach studied earlier, which proved rather successful in reproducing nucleon properties in nuclear matter obtained with more microscopical approaches.

We have obtained $Im\bar{\Sigma}$ for different values of the nuclear density and several temperatures. One of the interesting findings is that $Im\bar{\Sigma}$ grows steadily with the temperature. The changes produced by the temperature are more striking at energies around the chemical potential where $Im\bar{\Sigma}$ is zero at $T = 0$ and takes finite values at $T \neq 0$.

We found that the genuine effects of the temperature, given naturally in the formalism of Thermo Field Dynamics, were important, and the differences with respect to simple calculations, where $n(\vec{k})$ at $T = 0$ is replaced by the thermal distribution, can be appreciable. In order to facilitate the use of the results obtained here, we have parameterized them by means of easy analytical formulae. The parameterization is given for an effective NN cross section in the medium, such that $\sigma_{NN}^{eff}\ \rho$ gives the probability of collision per unit length for a nucleon in the nuclear medium. With the given formulae one can easily interpolate the results and obtain this magnitude for different densities and temperatures. These results should be useful in the analysis of heavy ion reactions.

Acknowledgements

We would like to thank Liang-gang Liu and Igor Tkachenko for useful discussions. This work has been partly supported by CICYT contract number AEN 93-1205.

6 Table Captions

Table I Parameters of eq. (28) to evaluate $v\sigma_{NN}^{eff}$ at $\rho = \rho_0/2$. The parameters a_n have dimensions such that, with ω given in MeV, the results for $v\sigma_{NN}^{eff}$ are given in mb.

Table II Same as table I for $\rho = \rho_0$.

Table III Same as table I for $\rho = 2\rho_0$.

7 Figure Captions

Fig. 1. Generic Feynman diagram to evaluate the nucleon self-energy. The indices a, b, c, d are thermal indices. The nucleon propagator corresponding to the baryonic lines is given in eqs. (5-9).

Fig. 2. *a*) polarization, *b*) correlation graphs contributing to $Im\Sigma$ at $T = 0$ and contained in fig. 1. Here the direction of the arrows stands for the conventional hole (down) and particle (up) propagators.

Fig. 3. Polarization graphs appearing at $T = 0$ with the same notation for the lines as in fig. 2.

Fig. 4. $-Im\bar{\Sigma}(\omega, k)$ at $T = 0$ as a function of $\omega - \mu$, with $k = \sqrt{2M\omega}$, evaluated for two densities.

Fig. 5. $Im\Sigma^{(11)}(\omega, k)$ at $\rho = \rho_0$ for several temperatures as a function of $\omega - \mu$ with $k = \sqrt{2M\omega}$. The solid line is for $T = 0$. The other curves correspond to $T = 2\,MeV$ (long dashed-dotted line), $T = 4\,MeV$ (dashed line), $T = 10\,MeV$ (dotted line) and $T = 20\,MeV$ (short dashed-dotted line). At values $\omega - \mu < 0$, they appear correlatively with increasing values of $Im\Sigma^{(11)}$ as T increases.

Fig. 6. $-Im\bar{\Sigma}(\omega, k)$ at $\rho = \rho_0/2$ as a function of $\omega - \mu$ for $k = \sqrt{2M\omega}$ for several temperatures $T = 0, 2, 4, 10, 20\,MeV$ with the same notation as in fig. 5. $-Im\bar{\Sigma}$ increases with increasing T.

Fig. 7. Same as fig. 6 at $\rho = \rho_0$.

Fig. 8. Same as fig. 6 at $\rho = 2\rho_0$.

References

[1] C. Mahaux, P. F. Bortignon, R. A. Broglia and C. H. Dasso, Phys. Rep. **120** (1985) 1, and refs. therein.

[2] R. B. Clare and D. Strottman, Phys. Rep. **141** (1986) 177

[3] T. Matsubara, Prog. Theor. Phys. **14** (1955) 351.

[4] A. L. Fetter and J. D. Walecka, Quantum Theory of Many Particle Systems (McGraw-Hill, New York, 1971).

[5] L. Leplae, H. Umezawa and F. Mancini, Phys. Rep. **10** (1974) 151.

[6] T. Arimitsu and H. Umezawa, Prog. Theor. Phys. **77** (1987) 32 and 53.

[7] P. A. Henning, Phys. Rep. **253** (1995) 235.

[8] R. J. Furnstahl and B. D. Serot, Phys. Rev. **C43** (1991) 105

[9] B. D. Serot and J. D. Walecka, Adv. Nucl. Phys. **16** (1986) 1.

[10] A. Lejeune, P. Granje, M. Martzolff and J. Cugnon, Nucl. Phys. **A453** (1986) 189.

[11] P. Grange, J. Cugnon and A. Lejeune, Nucl. Phys. **A473** (1987) 365.

[12] J. Helgesson and J. Randrup, Ann. of Phys. (N.Y.) in print

[13] P. Fernández de Córdoba and E. Oset, Phys. Rev. **C46** (1992) 1697.

[14] C. B. Dover, J. Hüfner and R. H. Lemmer, Ann. of Phys. (N.Y.) **66** (1971) 248.

[15] J. Hüfner, Phys. Rep. **21** (1975) 1.

[16] S. Fantoni, B. L. Friman and V. R. Pandharipande, Nucl. Phys. **A399** (1983) 51.

[17] S. Fantoni and V. R. Pandharipande, Nucl. Phys. **A427** (1984) 473.

[18] A. Ramos, A. Polls and W.H. Dickhoff, Nucl. Phys. **A503** (1989) 1.

[19] K. Saito, T. Maruyana and K. Soutome, Phys. Rev. **C40** (1989) 407.

[20] J. Cugnon, A. Lejeune, M. Baldo and K. Lombardo, Nucl. Phys. **A492** (1989) 173.

[21] G. E. Brown, Many Body Problems (North-Holland Amsterdam, 1972)

[22] G. Baym and C. Pethick, Landau Fermi-Liquid Theory, John Wiley and Sons, 1991, pag. 87.

[23] G.E. Brown, E. Oset, M.J. Vicente-Vacas and W. Weise, Nucl. Phys. **A505** (1989) 823.

Table I.

T / a_n	0 MeV	2 MeV	4 MeV	10 MeV	20 MeV
a_0	-2.549	-2.305	-1.425	0.982	5.107
a_1	$9.658\ 10^{-2}$	$9.098\ 10^{-2}$	$7.043\ 10^{-2}$	$3.404\ 10^{-2}$	$-2.170\ 10^{-2}$
a_2	$-9.706\ 10^{-5}$	$-3.996\ 10^{-5}$	$1.569\ 10^{-4}$	$4.367\ 10^{-4}$	$8.413\ 10^{-4}$
a_3	$-4.349\ 10^{-7}$	$-6.674\ 10^{-7}$	$-1.435\ 10^{-6}$	$-2.408\ 10^{-6}$	$-3.857\ 10^{-6}$
a_4	$1.135\ 10^{-9}$	$1.456\ 10^{-9}$	$2.487\ 10^{-9}$	$3.724\ 10^{-9}$	$5.709\ 10^{-9}$

Table II.

T / a_n	0 MeV	2 MeV	4 MeV	10 MeV	20 MeV
a_0	0.553	0.411	0.793	1.695	3.192
a_1	$-3.541\ 10^{-2}$	$-2.722\ 10^{-2}$	$-3.709\ 10^{-2}$	$-4.496\ 10^{-2}$	$-4.430\ 10^{-2}$
a_2	$7.790\ 10^{-4}$	$6.834\ 10^{-4}$	$7.846\ 10^{-4}$	$8.343\ 10^{-4}$	$7.542\ 10^{-4}$
a_3	$-2.860\ 10^{-6}$	$-2.458\ 10^{-6}$	$-2.861\ 10^{-6}$	$-3.027\ 10^{-6}$	$-2.651\ 10^{-6}$
a_4	$3.521\ 10^{-9}$	$2.963\ 10^{-9}$	$3.501\ 10^{-9}$	$3.719\ 10^{-9}$	$3.215\ 10^{-9}$

Table III.

T / a_n	0 MeV	2 MeV	4 MeV	10 MeV	20 MeV
a_0	1.493	1.382	1.347	2.205	2.861
a_1	$-5.370\ 10^{-2}$	$-5.017\ 10^{-2}$	$-4.795\ 10^{-2}$	$-6.283\ 10^{-2}$	$-6.065\ 10^{-2}$
a_2	$5.866\ 10^{-4}$	$5.555\ 10^{-4}$	$5.355\ 10^{-4}$	$6.533\ 10^{-4}$	$6.214\ 10^{-4}$
a_3	$-1.659\ 10^{-6}$	$-1.553\ 10^{-6}$	$-1.484\ 10^{-6}$	$-1.874\ 10^{-6}$	$-1.770\ 10^{-6}$
a_4	$1.695\ 10^{-9}$	$1.570\ 10^{-9}$	$1.488\ 10^{-9}$	$1.940\ 10^{-9}$	$1.834\ 10^{-9}$

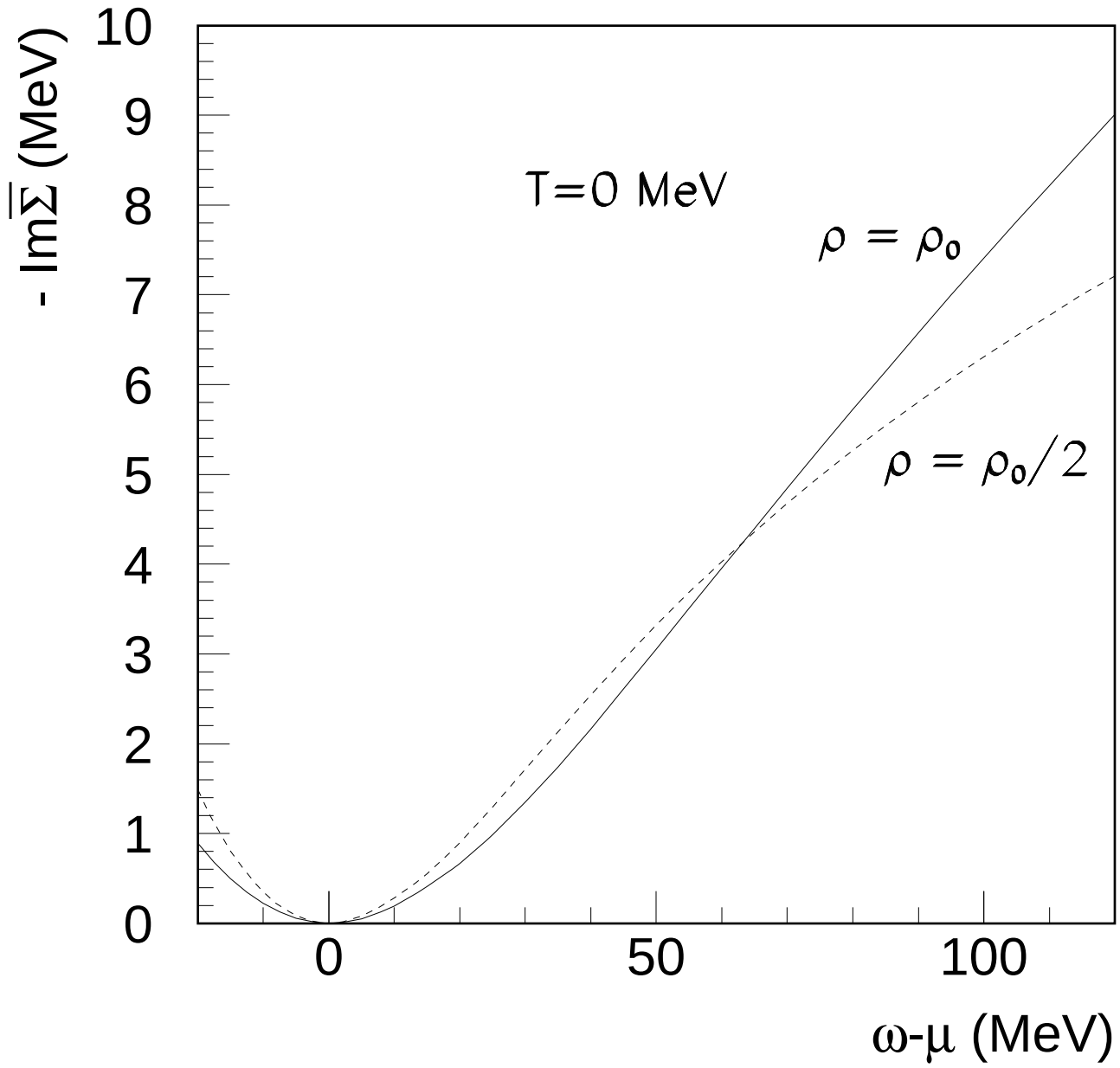
- Im$\bar{\Sigma}$ (MeV)
10
9
8
7
6
5
4
3
2
1
0
T=0 MeV
$\rho = \rho_0$
$\rho = \rho_0/2$
0
50
100
ω-μ (MeV)

Fig. 4

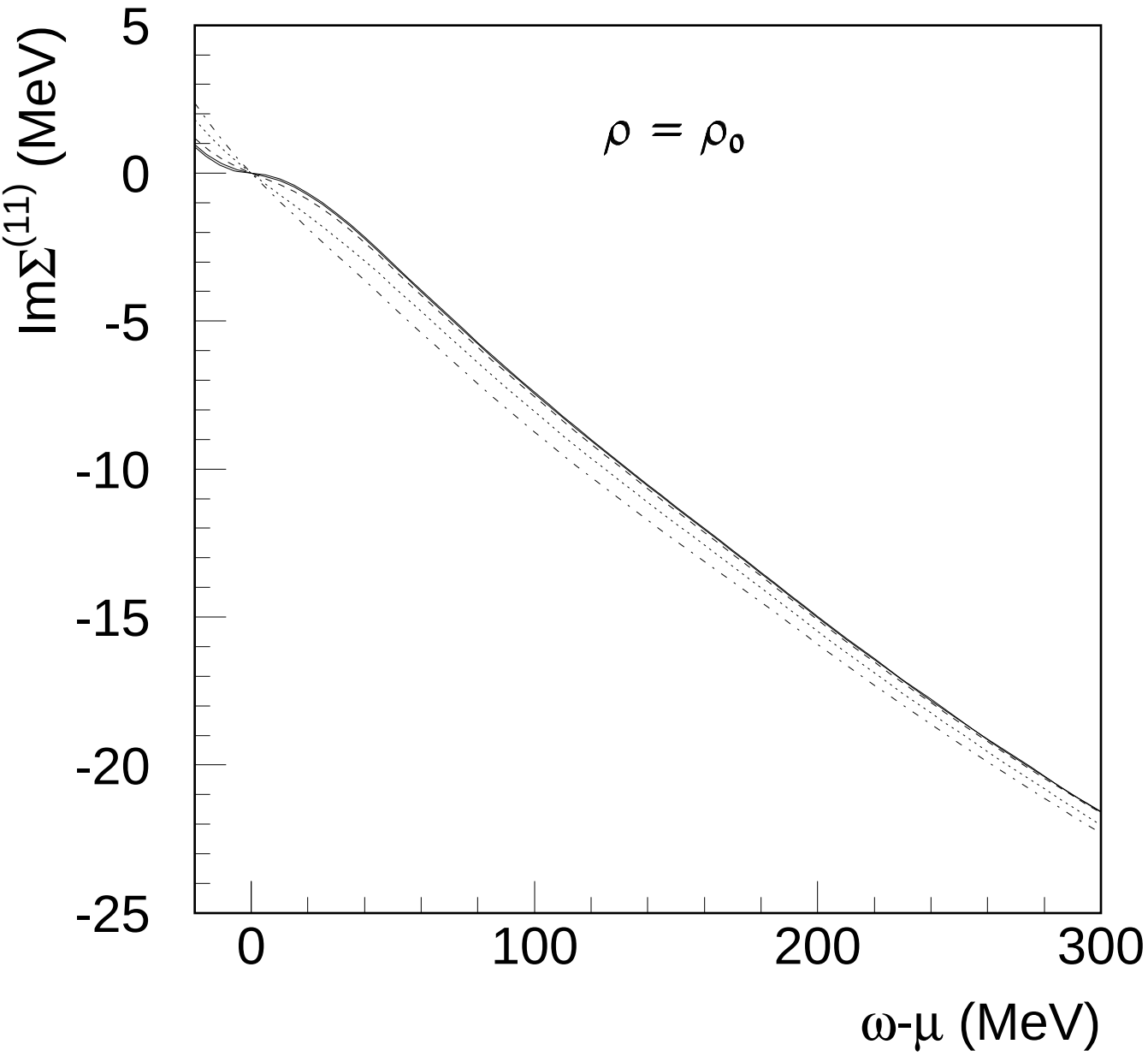
$\rho = \rho_0$
$\mathrm{Im}\Sigma^{(11)}$ (MeV)
5
0
-5
-10
-15
-20
-25
0
100
200
300
ω-μ (MeV)

Fig. 5

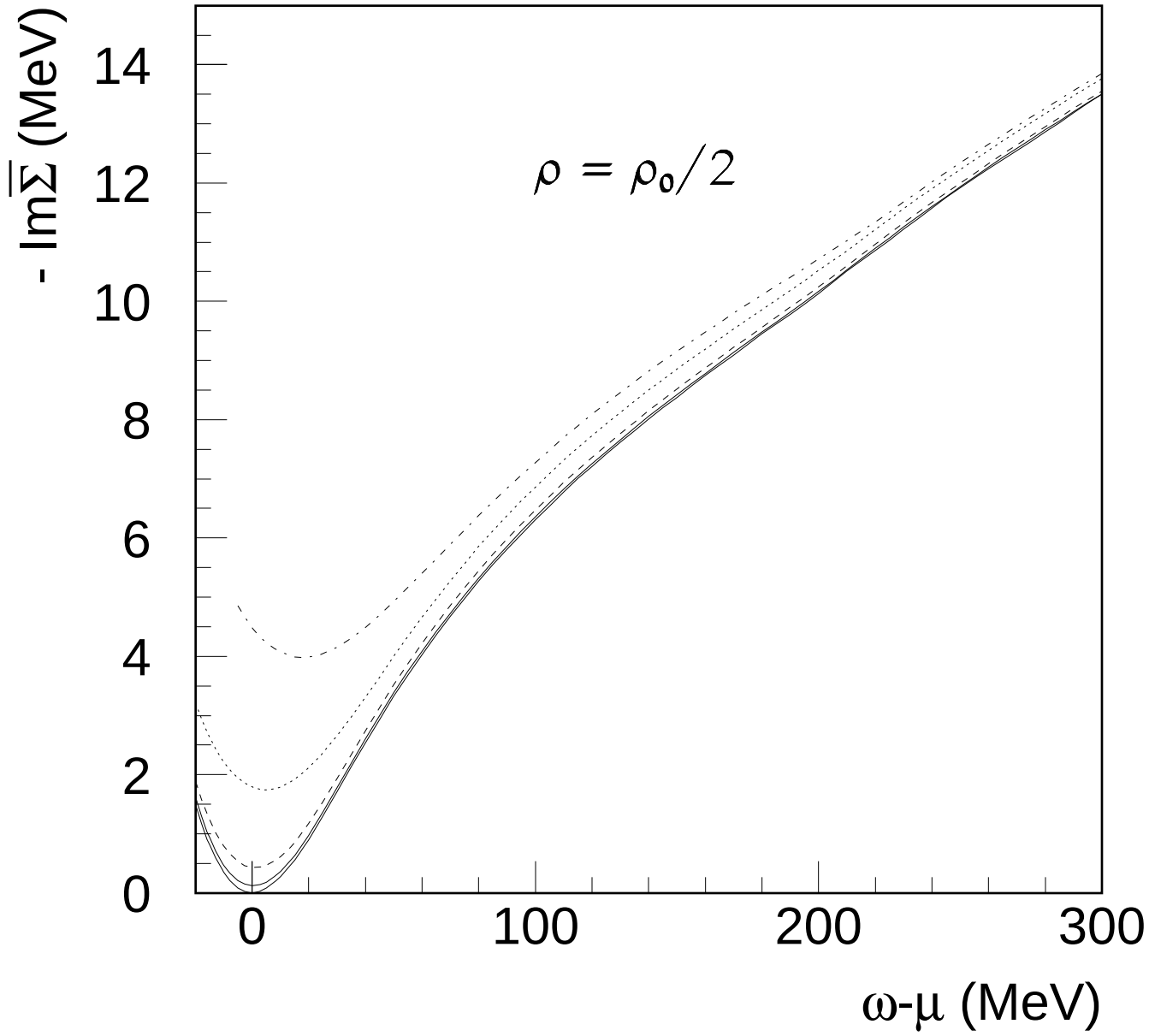

Fig. 6

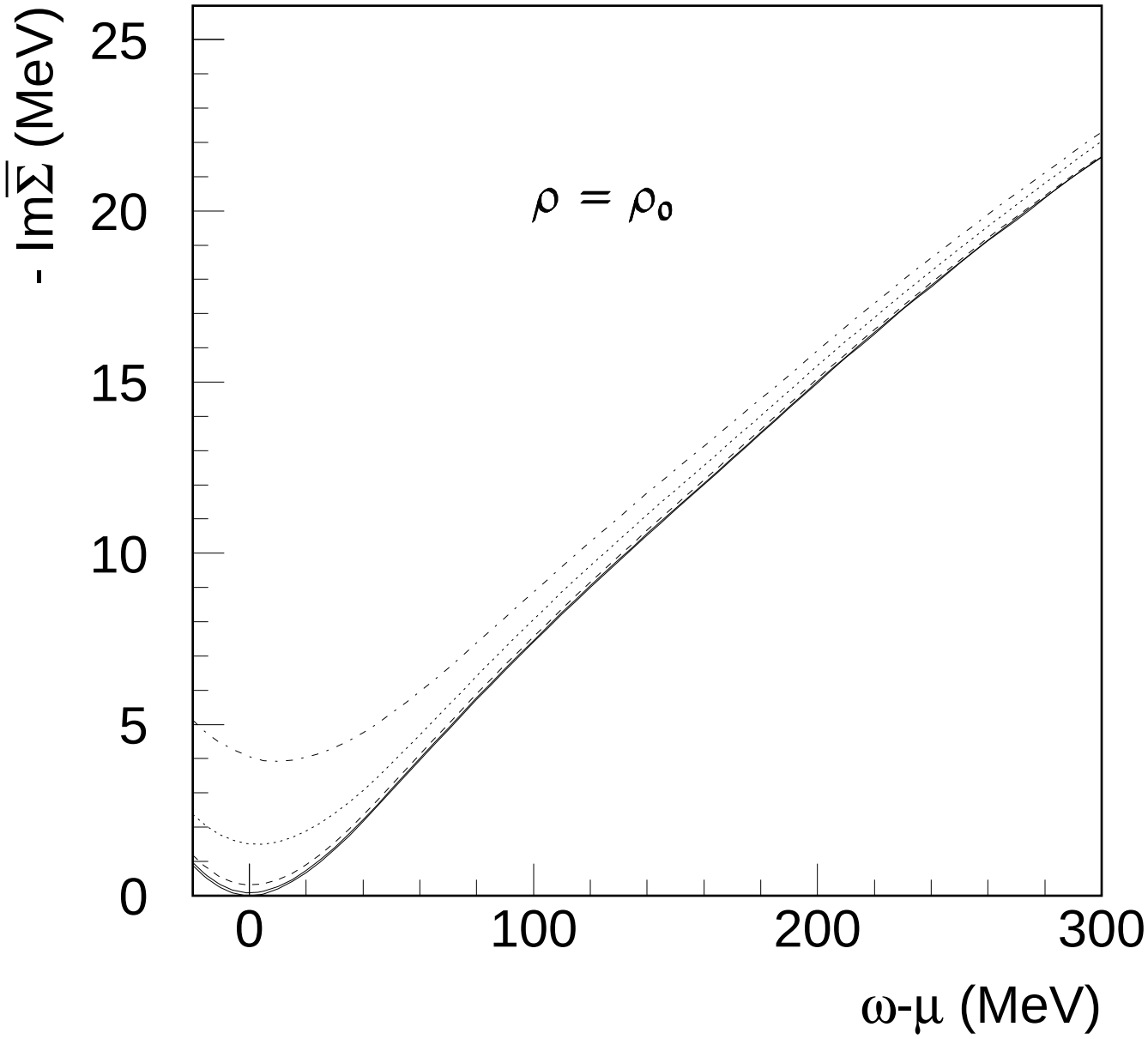

Fig. 7

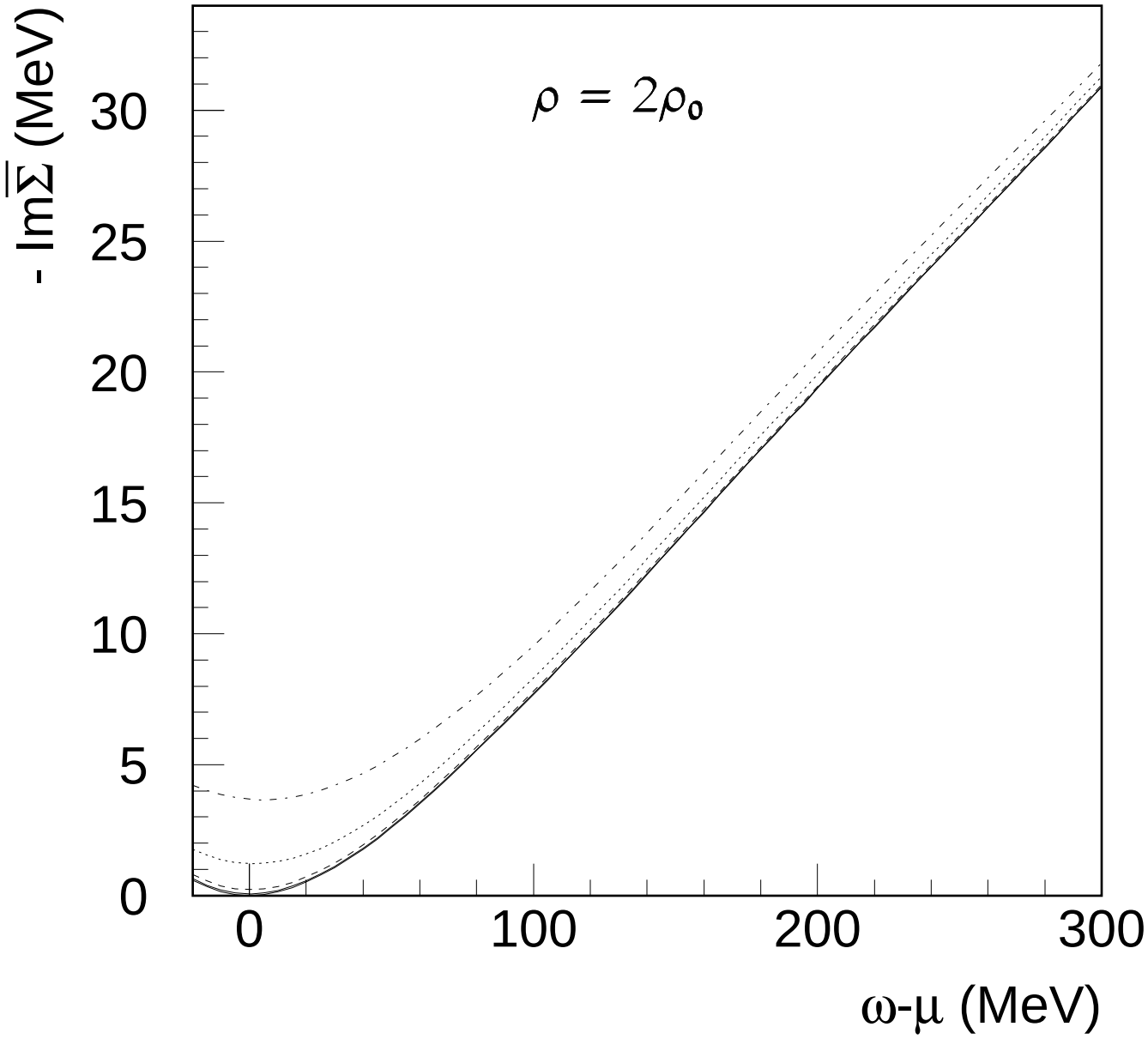

Fig. 8

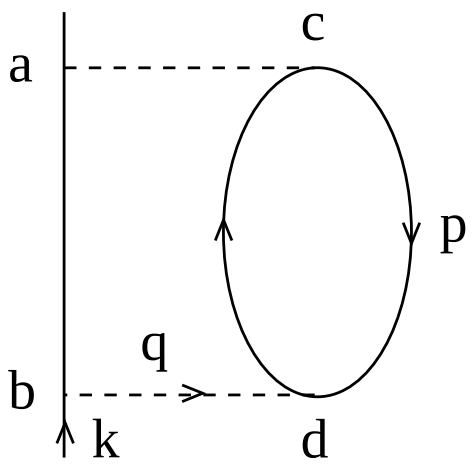

Fig 1

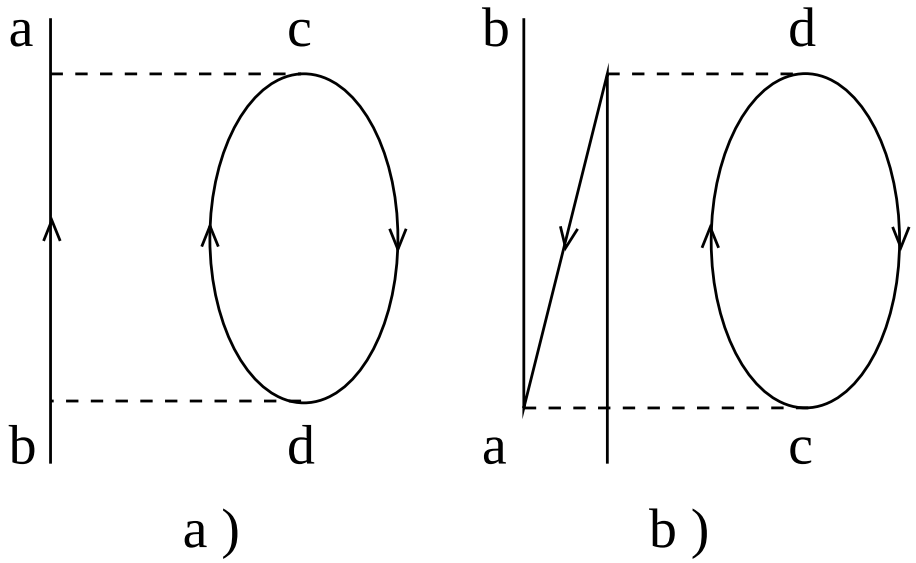

Fig 2

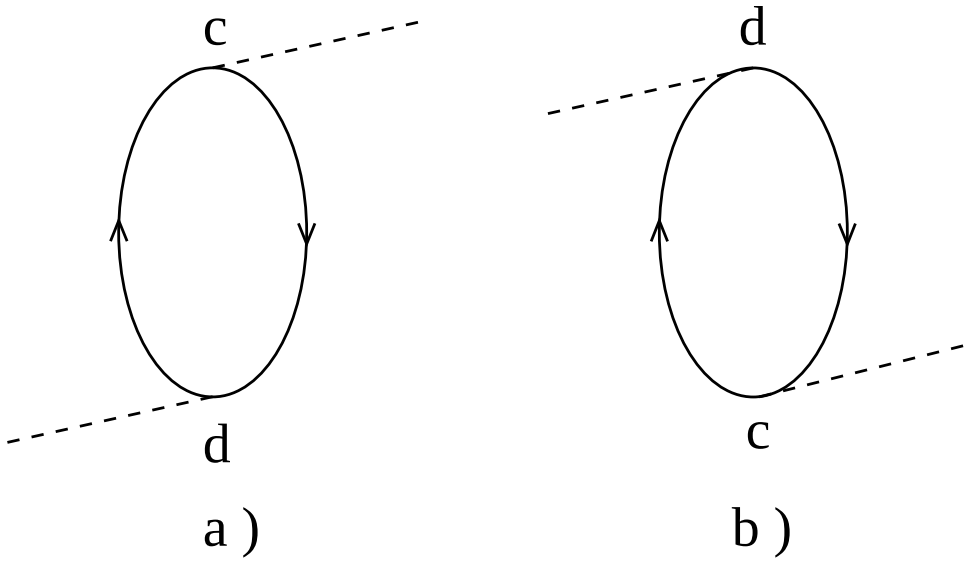

Fig 3